

Performance comparison of *p*-side-up thin-film AlGaInP light emitting diodes with aluminum-doped zinc oxide and indium tin oxide transparent conductive layers

Ming-Chun Tseng,¹ Dong-Sing Wu,^{1,5} Chi-Lu Chen,² Hsin-Ying Lee,³ Yu-Chang Lin,³ and Ray-Hua Horng^{2,4,*}

¹Department of Materials Science and Engineering, National Chung Hsing University, Taichung 402, Taiwan

²Graduate Institute of Precision Engineering, National Chung Hsing University, Taichung 402, Taiwan

³Department of Photonics, National Cheng Kung University, Tainan 701, Taiwan

⁴Department of Electronics Engineering, Chiao Tung University, Hsinchu 300, Taiwan

⁵Advanced Optoelectronic Technology Center, National Cheng Kung University, Tainan 701, Taiwan

*rhh@nctu.edu.tw

Abstract: Transparent conductive layers (TCLs) deposited on a GaP window layer were used to fabricate high-brightness *p*-side-up thin-film AlGaInP light-emitting diodes (LEDs) by the twice wafer-transfer technique. Indium tin oxide (ITO) and aluminum-doped zinc oxide (AZO) were used as TCLs for comparison. The TCLs improved droop of external quantum efficiencies (EQE) of LEDs and junction temperature, which result in increasing the light output power and thermal stability of the LEDs. The droop efficiency of Ref-LED, ITO-LED and AZO-LED were 64%, 27% and 15%, respectively. The junction temperature of ITO-LED and AZO-LED reduced to 49.3 and 39.6 °C at an injection current of 700 mA compared with that (80.8 °C) of Ref-LED. The LEDs with AZO layers exhibited the most excellent LED performance. The emission wavelength shifts of LEDs without a TCL, with an ITO layer, and with an AZO layer were 17, 8, and 3 nm, respectively, when the injection current was increased from 20 to 1000 mA. The above results are promising for the development of AZO thin films to replace ITO thin films for AlGaInP LED applications.

©2016 Optical Society of America

OCIS codes: (230.0230) Optical devices; (230.3670) Light-emitting diodes.

References and links

1. S. C. Hsu, D. S. Wu, C. Y. Lee, J. Y. Su, and R. H. Horng, "High-efficiency 1 mm² AlGaInP LEDs sandwiched by ITO omni-directional reflector and current-spreading layer," *IEEE Photonics Technol. Lett.* **19**(7), 492–494 (2007).
2. R. H. Horng, B. R. Wu, C. F. Weng, P. Ravadgar, T. M. Wu, S. P. Wang, J. H. He, T. H. Yang, Y. M. Chen, T. C. Hsu, A. S. Liu, and D. S. Wu, "P-side up AlGaInP-based light emitting diodes with dot-patterned GaAs contact layers," *Opt. Express* **21**(17), 19668–19674 (2013).
3. Y. J. Lee, H. C. Kuo, S. C. Wang, T. C. Hsu, M. H. Hsieh, M. J. Jou, and B. J. Lee, "Increasing the extraction efficiency of AlGaInP LEDs via n-side surface roughening," *IEEE Photonics Technol. Lett.* **17**(11), 2289–2291 (2005).
4. K. Bergenek, C. Wiesmann, R. Wirth, L. O'Faolain, N. Linder, K. Streubel, and T. F. Krauss, "Enhanced light extraction efficiency from AlGaInP thin-film light-emitting diodes with photonic crystals," *Appl. Phys. Lett.* **93**(4), 041105 (2008).
5. M. R. Krames, M. Ochiai-Holcomb, G. E. Höfler, C. Carter-Coman, E. I. Chen, I. H. Tan, P. Grillot, N. F. Gardner, H. C. Chui, J. W. Huang, S. A. Stockman, F. A. Kish, M. G. Craford, T. S. Tan, C. P. Kocot, M. Hueschen, J. Posselt, B. Loh, G. Sasser, and D. Collins, "High-power truncated-inverted-pyramid (Al_{1-x}Ga_x)_{0.5}In_{0.5}P/GaP light-emitting diodes exhibiting >50% external quantum efficiency," *Appl. Phys. Lett.* **75**(16), 2365–2367 (1999).
6. M. C. Tseng, C. L. Chen, N. K. Lai, S. I. Chen, T. C. Hsu, Y. R. Peng, and R. H. Horng, "P-side-up thin-film AlGaInP-based light emitting diodes with direct ohmic contact of an ITO layer with a GaP window layer," *Opt. Express* **22**(S7 Suppl 7), A1862–A1867 (2014).

7. C. H. Yen, Y. J. Liu, K. H. Yu, P. L. Lin, T. P. Chen, L. Y. Chen, T. H. Tsai, N. Y. Huang, C. Y. Lee, and W. C. Liu, "On an AlGaInP-based light-emitting diode with an ITO direct ohmic contact structure," *IEEE Electron Device Lett.* **30**(4), 359–361 (2009).
8. S. M. Pan, R. C. Tu, Y. M. Fan, R. C. Yeh, and J. T. Hsu, "Enhanced output power of InGaN–GaN light-emitting diodes with high-transparency nickel-oxide–indium-tin-oxide ohmic contacts," *IEEE Photonics Technol. Lett.* **15**(5), 646–648 (2003).
9. K. Ellmer, A. Klein, and B. Rech, *Transparent Conductive Zinc Oxide* (Springer, 2008), Chap 1.
10. R. H. Horng, K. C. Shen, C. Y. Yin, C. Y. Huang, and D. S. Wu, "High performance of Ga-doped ZnO transparent conductive layers using MOCVD for GaN LED applications," *Opt. Express* **21**(12), 14452–14457 (2013).
11. S. J. Chang, X. F. Zeng, S. C. Shei, and S. Li, "AlGaInP-based LEDs with AuBe-diffused AZO/GaP current spreading layer," *IEEE J. Quantum Electron.* **49**(10), 846–851 (2013).
12. C. C. Liu, W. T. Wang, M. P. Hwang, Y. H. Wang, and S. M. Chen, "Titanium nitride as spreading layers for AlGaInP visible LEDs," *IEEE Photonics Technol. Lett.* **14**(12), 1665–1667 (2002).
13. E. Matioli and C. Weisbuch, "Direct measurement of internal quantum efficiency in light emitting diodes under electrical injection," *J. Appl. Phys.* **109**(7), 073114 (2011).
14. E. F. Schubert, *Light-Emitting Diodes*, 2nd ed. (Cambridge University Press, 2006), chap. 8.

1. Introduction

Quaternary $(\text{Al}_{1-x}\text{Ga}_x)_{0.5}\text{In}_{0.5}\text{P}$ -based light-emitting diodes (LEDs) with red and yellow/green spectra have received considerable attention. Although the external efficiency of AlGaInP LEDs is limited by the light absorption of the GaAs substrate and the narrow critical angle of total internal reflection at the semiconductor-air interface, the output power efficiency of AlGaInP LEDs has been obviously improved using the once or twice wafer-transferring technique to overcome the light absorption problem by the GaAs substrate [1,2]. Nevertheless, the external quantum efficiency of AlGaInP LEDs is still limited by light extraction. Most photons are trapped inside the LED chip in a guided mode, which results from the large difference in the refractive indices between the semiconductor and epoxy for the packaged AlGaInP LEDs.

To solve this problem, several methods have been proposed, such as surface texturing [3], using photonic crystals [4], changing the cavity geometry [5], and applying auxiliary transparent conductive layers (TCLs) on the GaP window layer [6]. Recently, indium tin oxide (ITO) as a TCL has been proven to be one of the most promising materials for enhancing light extraction in AlGaInP-based LEDs because of its excellent conductivity and optical transparency in the visible wavelength range [7]. However, it is chemically unstable, toxic, rare, and expensive. The low thermal stability of ITO results in poor LED device reliability [8], which has led to the development of replacements for ITO. ZnO-based materials have been increasingly used as an alternative TCL in high-efficiency LEDs because of their excellent properties, such as superior thermal stability, favorable electronic and optical properties (similar to those of ITO), and lower cost of fabrication than that of ITO [9].

In our previous study, Ga-doped ZnO directly contacted with *p*-type GaN and acted as the TCL after thermal treatment [10]. Furthermore, S. Chang *et al.* [11] reported AlGaInP-based LEDs with an AZO/GaP current spreading layer. Nevertheless, the deposition and diffusion of AuBe into the *p*-GaP layer before the AZO deposition was necessary. Up to now, a ZnO-based TCL directly contacted with *p*-GaP for thin-film AlGaInP LED applications has not been reported.

In this study, AlGaInP LEDs with a thin carbon-doped GaP cap layer were transferred onto a Si substrate with mirror structure (i.e. Ag-reflector) using the twice wafer-transfer technique to construct *p*-side-up thin-film AlGaInP LEDs with vertical metal contacts. We note that the thin film AlGaInP LEDs presented the *p*-side up structure, i.e., the GaP cap layer still acts as the window layer and contributes to light extraction. Moreover, a Si substrate with mirror structure has been used instead of a GaAs absorbing substrate by the twice wafer-transfer technique. The TCLs (ITO and AZO thin films) achieved ohmic contact with the thin carbon-doped GaP cap layer. The electrical properties of *p*-side-up thin-film AlGaInP LEDs with ITO and AZO thin films used as current spreading layers to enhance the light extraction efficiency are compared and described in detail.

2. Experimental details

The AlGaInP LED epilayers were grown on *n*-type GaAs substrates by metal-organic chemical vapor deposition. As shown in Fig. 1(a), the structure consists of a carbon-doped p^+ -GaP ohmic contact layer, p -GaP:Mg window layer, p -cladding AlGaInP, GaInP-AlGaInP MQWs, n -cladding AlGaInP, n^+ -GaAs contact layer, and GaInP etching stop layer. Twice wafer-transfer technology procedures have been described in our previous studies [6]. It is worth mentioning that Cr/Au/In metals not only acted as the bonding layers, but also as an ohmic contact with n^+ -type Si substrate, shown in Fig. 1(b). The front grid metal Ti/Al/Ti/Au (25/2000/50/100 nm) was deposited on top of the TCL to act as the p -contact pads, and the bottom electrode Ti/Au (5/100 nm) was deposited on the rear of the Si substrate with the LED thin epilayer to act as the n -contact pads. Finally, all samples were cut into separated chips with dimensions of $1010 \times 1010 \mu\text{m}^2$. As concerning the TCL layer, the AZO thin film was deposited on a p -side-up thin-film AlGaInP LED with a Zn:Al cycle ratio of 20:1 by using atomic layer deposition (ALD). The deposition temperature and pressure were 200°C and 0.6 Torr, respectively. Diethylzinc [$\text{Zn}(\text{C}_2\text{H}_5)_2$, DEZ], trimethylaluminum [$\text{Al}(\text{CH}_3)_3$], and de-ionized water were used as Zn, Al, and O precursors for depositing the AZO thin film with a growth rate of 0.14 nm/cycle. Al was doped into the ZnO film by introducing the Al precursor into the reaction chamber once during all 20 cycles of DEZ injections. The ITO thin film was deposited by electron gun evaporator at 300°C . To evaluate the effects of the AZO contact layer on the LED performance, three types of LEDs were fabricated using the same epilayers. One is Ref-LED; p -side-up thin-film AlGaInP LED with a AuBe/Au p -contact layer. Another is p -side-up thin-film AlGaInP LED with ITO current spreading layer (ITO-LED). The other is p -side-up thin-film AlGaInP LED with AZO current spreading layer (AZO-LED).

The current-voltage (I-V) characteristics of these LEDs were measured at room temperature using an Agilent 4155B semiconductor parameter analyzer. The refractive indices of the TCLs were measured using an n&k Technology model 1280 analyzer, which performs real-time non-destructive characterization of the optical properties of thin film materials. The light output power and thermal behaviors (Junction temperature) were measured by TERALED & T3Ster Combined System. Moreover, each optoelectronic characteristic result shown in this research was obtained from the average data measured 50 different samples.

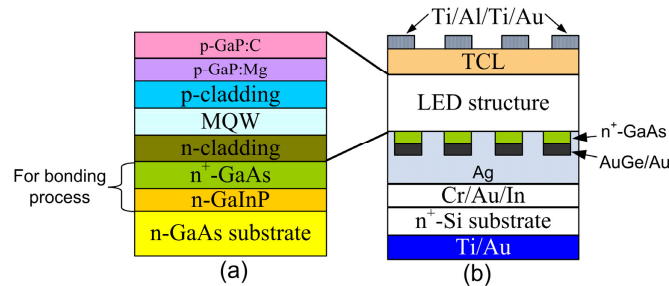


Fig. 1. Schematic diagrams of (a) p -side up AlGaInP-based LED structure, (b) p -side up thin film AlGaInP-based LED with TCL contact layer after twice wafer-transferring technique.

3. Results and discussion

Figure 2 shows the contact characteristics of AuBe/Au, the ITO thin film, and the AZO thin film contacted with the p -GaP:C cap layer. The schematic diagram of contact characteristics for pad-to-pad measurement is shown in the insert of Fig. 2(a). The ITO thin film can directly contact with the p -GaP:C cap layer without post-annealing due to heavily carbon-doped GaP layer [6]. The AZO thin film in contact with the p -GaP:C cap layer showed nonlinear current-voltage (I-V) behavior before annealing. To evaluate the contact resistance of TCL contacted to p -GaP:C, the AZO thin film was annealed at 350°C for 1 minute under N_2 ambient and

ITO thin film without post annealing for comparison with AuBe/Au deposited on a *p*-GaP:C layer using 550°C annealing for 30 seconds. The contact characteristics of annealed Au/AuBe/*p*-GaP:C, ITO/*p*-GaP:C, and annealed AZO/*p*-GaP:C showed linear I-V characteristics. The resistance of pad-to-pad Au/AuBe/*p*-GaP:C was lower than those of ITO/*p*-GaP:C and AZO/*p*-GaP:C. Moreover, the resistance of pad-to-pad annealed AZO/*p*-GaP:C was similar to that of ITO/*p*-GaP:C.

To study the contact properties of the ITO and AZO thin films on the *p*-GaP:C cap layer, the circular transmission line model (CTLM) was used to evaluate the specific contact resistances (ρ_c) and sheet resistance (R_s). The CTLM results of TCLs/*p*-GaP:C and Au/AuBe/*p*-GaP:C were shown in resistance versus distance and displayed in Fig. 2(b). In this work, both of the ρ_c and R_s were extracted from the CTLM results. The specific contact resistance of *p*-Au/AuBe/*p*-GaP:C with 550 °C post annealing was $7.7 \times 10^{-5} \Omega \cdot \text{cm}^2$. In addition, the specific contact resistances of the ITO/*p*-GaP:C and AZO/*p*-GaP:C were 2.6×10^{-3} and $6.6 \times 10^{-3} \Omega \cdot \text{cm}^2$, respectively. It is worth mentioning that the ρ_c and R_s of AZO/*p*-GaP:C are a little higher than those of ITO/*p*-GaP:C. Moreover, as compared with the ρ_c ($1.54 \times 10^{-4} \Omega \cdot \text{cm}^2$) of AZO on AuBe diffused GaP (ref. 11), the ρ_c of AZO/*p*-GaP:C is higher than that reported by Ref.11.

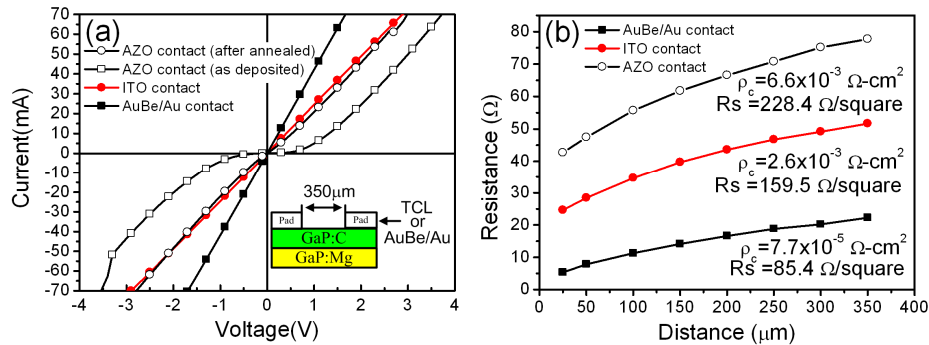


Fig. 2. (a) I-V behaviors of *p*-GaP:C/AuBe/Au with 550°C post annealing, *p*-GaP:C without annealing and AZO/*p*-GaP:C before and after 350°C post annealing and (b) CTLM results of Au/AuBe/*p*-GaP:C, ITO/*p*-GaP:C and AZO/*p*-GaP:C.

In order to study the contact behavior of AZO on the *p*-GaP:C cap layer, the AZO thin film first was deposited on the *p*-GaP:C cap layer surface and annealed by RTA at 350°C, then the AZO thin film was removed from *p*-GaP:C surface. Subsequently, the *p*-GaP:C surface was measured by X-ray photoelectron spectroscopy (XPS). The XPS spectra of Ga2*p* at the *p*-GaP surface of the bare *p*-GaP surface and after annealing (350 °C) are shown in Fig. 3. The surface Fermi level shift in *p*-GaP was determined using the energy position of the Ga2*p* core level peaks in the XPS spectra. This is one of the most accurate methods of determining the shift in the Fermi level position. The Ga2*p* core level peak at the *p*-GaP surface after annealing at 350 °C shifted from 1116.8 to 1116.6 eV. This means that the Fermi level shifted toward the valence band edge through Zn diffusion, resulting in a reduction in the barrier height of the *p*-GaP surface. A peak shift indicates an increase in the concentration at the *p*-GaP:C surface. Furthermore, the contact resistance of the AZO thin film on *p*-GaP:C obtained using the CTLM was considerably decreased from Schottky contact to $6.6 \times 10^{-3} \Omega \cdot \text{cm}^2$ (ohmic contact) after the RTA process. This can explain the ohmic contact characteristics of the annealed (350 °C) AZO/*p*-GaP:C sample.

A major concern as regarding the *p*-side-up thin-film AlGaInP LEDs with a TCL deposited on the *p*-GaP window layer is their I-V characteristics. The forward I-V characteristics of Ref-, TCL-LEDs are shown in Fig. 4. All LED structures exhibited normal *p*-*n* diode behaviors at a forward dc bias, shown in Fig. 4(a). At a current injection of 350 mA, the forward voltages of Ref-LED, ITO-LED, and AZO-LED were 2.54, 2.21, and 2.41 V, respectively. The forward voltage of the AZO-LED was lower than that of Ref-LED, but

higher than that of ITO-LED. Because the TCLs were deposited on the entire *p*-GaP window layer, they can act as not only an ohmic contact layer but also a current spreading layer in which current is injected from the top contact metal through the TCL to the entire active layer of the LED. However, the contact resistance of the AZO thin film was higher than that of the ITO thin film (shown in Fig. 2(b)), which resulted in the higher forward voltage of the LED. The dynamic resistances of these three LEDs as a function of the applied voltage were shown in Fig. 4(b). When the applied voltage was higher than 1.7 V, lower dynamic resistances were obtained for the TCL-LEDs than that for the Ref-LED. The dynamic resistances of Ref-LED, ITO-LED, and AZO-LED were 1.26, 0.83, and 0.85Ω, respectively, at an applied voltage of 2.5 V. The dynamic resistances of the AZO-LED were lower than that of the Ref-LED and higher than that of the ITO-LED. Figure 4(c) shows typical reverse I-V characteristics for Ref-LED, ITO-LED and AZO-LED. The current variation with no apparent breakdown was obtained. For comparison, the reverse current is 1.18×10^{-7} , 2.44×10^{-8} and 2.34×10^{-8} A at a reverse voltage of -5 V for Ref-LED, ITO-LED and AZO-LED, respectively. The leakage current of AZO-LED was slightly lower than that of ITO-LED under reverse bias from 0 to -5 V. The electrical performance of AZO-LED indicated that they are better than those of Ref-LED and similar to those of ITO-LED even the contact resistance of AZO/*p*-GaP presented a little higher than that of ITO/*p*-GaP.

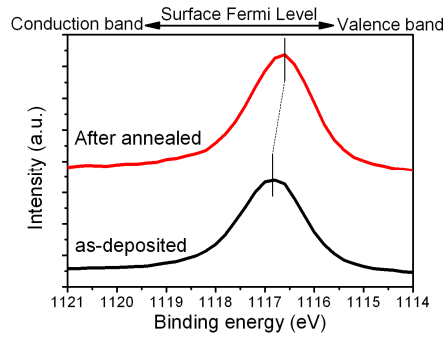


Fig. 3. XPS spectra of Ga2*p* core level for *p*-GaP surface before and after annealing process, the dotted line indicates a shift of the Ga2*p* core level.

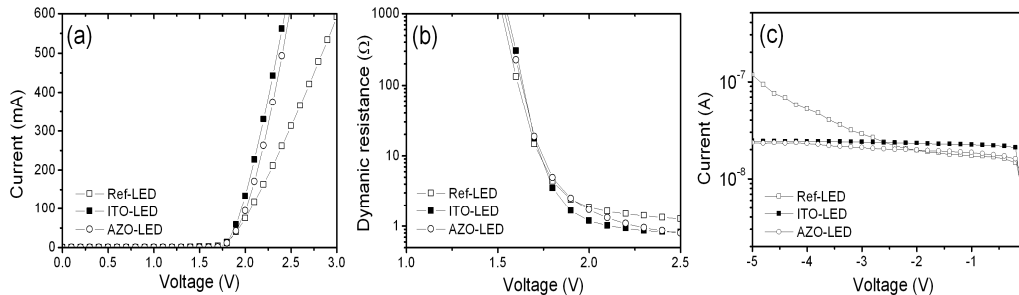


Fig. 4. (a) Forward I-V, (b) dynamic resistance characteristics and (c) leakage current in reverse voltage bias for Ref-, ITO- and AZO-LEDs.

Figure 5(a) illustrates the output power of the LEDs (with epoxy package) as a function of the injection current measured at room temperature. According to Fig. 5(a), all LED structures exhibited a linear relationship between the injection current and output power before an injection current of 700 mA. Moreover, ITO-LED and AZO-LED exhibited stable output powers at high injection currents (>700 mA) because of alleviation of the crowding effect near the *p*-pad metal. Although, the ohmic contact resistance of the Au/AuBe/ *p*-GaP:C electrode was lower than those of ITO/*p*-GaP:C and AZO/*p*-GaP:C, the output power of Ref-

LED decreased because of the accumulation of Joule heat [12], which was generated from the current crowding. In addition, using ITO and AZO thin films in AlGaInP-based LEDs not only effectively improved the current spreading effect to reduce the accumulation of Joule heat, but also increased the output powers. According to the results, the output power of AZO-LED was higher than that of ITO-LED. The output powers of Ref-LED, ITO-LED, and AZO-LED were 232, 290, and 370 mW at an injection current of 700 mA, and 180, 390, and 490 mW at an injection current of 1000 mA, respectively. The output powers of ITO-LED and AZO-LED increased by 25% and 59% at an injection current of 700 mA and 117% and 172% at an injection current of 1000 mA, respectively, compared with that of the Ref-LED. It is worth mentioning that AZO-LED presented the best output power performance even though it did not have the best I-V characteristics.

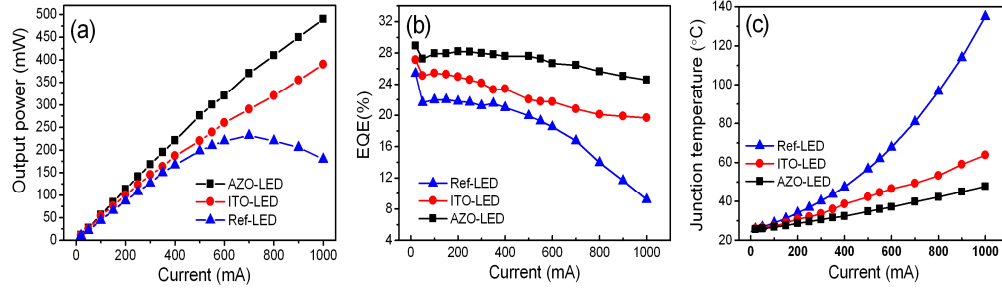


Fig. 5. (a) Output power characteristics, (b) EQE and (c) junction temperature for Ref-, ITO- and AZO-LEDs.

Based on the above results, evaluation of the light extraction efficiency (η_{extrac}) for these three types LEDs is important. The external quantum efficiencies (EQE) as a function of injection current are shown in Fig. 5(b). The external quantum efficiencies of Ref-LED, ITO-LED, and AZO-LED were 25%, 27%, and 29% at an injection current of 20 mA, respectively (Fig. 5(b)). In addition, the droop efficiencies (Definition: $[(EQE_{\text{max}} - EQE_{\text{min}}) / EQE_{\text{max}}] \times 100\%$) of Ref-LED, ITO-LED, and AZO-LED were 64%, 27%, and 15%, respectively. The droop efficiency obviously was improved by introducing the ITO and AZO thin films, especially for the LED with AZO layer. The internal quantum efficiency (IQE) is widely estimated by temperature-dependent photoluminescence (PL). The PL intensity of the emitted light at a certain PL excitation is measured at low temperature (LT), usually ~ 77 K and at room temperature (RT). The IQE is then estimated as the ratio of the peak PL intensities I_{RT} at room temperature and I_{LT} at low temperatures [13]. The IQE of the *p*-side-up AlGaInP LED was 98% after photoluminescence measurement (not shown). After calculation ($EQE = IQE \times \eta_{\text{extrac}}$), the η_{extrac} of Ref-, ITO- and AZO-LEDs were 26, 28 and 30%, respectively. There were 7% and 14% improved light extraction efficiencies for ITO- and AZO-LEDs than that of Ref-LED. This suggests that AZO can much more effectively extract light from GaP layer to epoxy than ITO does.

Figure 5(c) shows the junction temperature (T_j) as a function of the injection current of LEDs with Au/AuBe *p*-contact, ITO and AZO thin film. The junction temperature of Ref-LED, ITO-LED, and AZO-LED were 80.8, 49.3, and 39.6 °C at an injection current of 700 mA, and 135, 63.8, and 47.7 °C at an injection current of 1000 mA, respectively. The junction temperature of the LED was significantly improved by introduction of ITO and AZO thin films. The junction temperature of Ref-LED reveals an exponential increase, the increment in slope variation of junction temperature of Ref-LED was consistent with optoelectronic performance of Ref-LED decreased under high injection currents (>700 mA). Because most of the light was trapped inside the LED to increase accumulation of heat, which will further increase the junction temperature of LED device. The junction temperature of ITO-LED and AZO-LED change linearly with the increase in injection current, and the temperature sensitive coefficients (dT_j/dI) of ITO-LED and AZO-LED are 0.0388 °C/mA, and 0.0224

°C/mA, respectively. It was noticed that thermal stability of AZO-LED was better than those of the Ref-LED and ITO-LED. Furthermore, the lower junction temperature of an LED device means accumulation of Joule heat has been effectively reduced and more photons can escape from the LED surface.

Because the semiconductor energy gap is easily affected by temperature, the wavelength variation is another approach to evaluate the junction temperature of LEDs. Figure 6 shows the light emission wavelengths of Ref-, ITO-, and AZO-LEDs. The electroluminescence peaks of Ref-, ITO-, and AZO-LEDs were 617, 617, and 618 nm at an injection current of 20 mA, respectively. The wavelength red-shifts of Ref-, ITO-, and AZO-LEDs were approximately 17, 8, and 3 nm at an injection current of 20-1000 mA, respectively. The wavelength shift and corresponding junction temperature of LEDs with ITO and AZO thin films were lower than those of the Ref-LED because LEDs with ITO and AZO thin films provided more uniform current spreading than the Ref-LED with the AuBe/Au electrode. Obviously, LEDs with an AZO layer can provide the best output power and the lowest junction temperature. It results in the smallest wavelength variation.

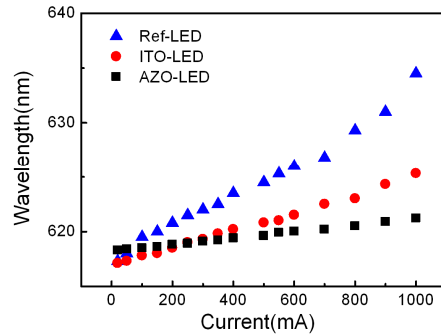


Fig. 6. Emission wavelengths of Ref-, ITO-, and AZO-LEDs with different injection current.

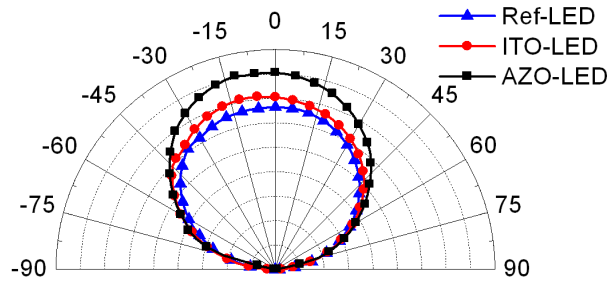


Fig. 7. Far-field radiation patterns of Ref-, ITO- and AZO-LEDs at the injection current of 350 mA.

Figure 7 illustrates far-field radiation patterns of Ref-, ITO-, and AZO-LEDs at an injection current of 350 mA. The output intensities of the LEDs with ITO and AZO thin films were higher than that of the Ref-LED regarding full angles because the refractive indices of ITO and AZO thin films are between those of the GaP layer ($n \approx 3.5$) and epoxy layer ($n \approx 1.5$). It is well known that the middle refractive index material inserted between the GaP layer and epoxy layer can minimize the total internal reflection effect. The optimal middle refractive index $(n_{GaP} \times n_{epoxy})^{1/2}$ is 2.29. However, this kind of material does not exist and it is difficult to achieve. The only solution is to find a material with a refractive index that is close to the optimal middle refractive index. The refractive indices of AZO and ITO thin films are approximately 2.20-1.80 in the wavelength range 320-1000 nm, between that of GaP and epoxy. The refractive indices of the ITO and AZO thin films in this study, measured using an n&k 1280 analyzer, were 1.85 and 2.00 at a wavelength of 610 nm, respectively. Therefore,

the critical angles of ITO-LED and AZO-LED increased from 16.6° to 31.9° and 34.8° , respectively, compared with the Ref-LED, to enhance the output intensities of the LED. In addition, the transmittance of the ITO thin film at a wavelength of 610 nm was 94%, which is higher than that of the AZO thin film (90%; spectrum not shown). Therefore, the main improvement in the performance of the AlGaInP-based LEDs with AZO layer could be attributed to the refractive index of the AZO. More light can escape from the surface of the LED, preventing the trapping of most photons inside the LED in a guided mode. The light extraction efficiency of the LEDs was improved, particularly in the normal direction. The results of the intensity in the normal direction (0° direction) are consistent with the optoelectronic performance of the LEDs with ITO and AZO thin films. The viewing angles of Ref-LED, ITO-LED, and AZO-LED were 129° , 123° , and 123° , respectively. More light was extracted from the surfaces of AZO-LED and ITO-LED than from those of Ref-LED, thus reducing the guiding mode light and finally resulting in a narrower viewing angle.

To understand the relevant optical properties and light intensity distribution properties on the LED chip surface, the near-field optical images were taken for these three samples. Near-field optical images of Ref-, ITO-, and AZO-LEDs at the same injection current are shown in Fig. 8. The output light intensity distribution and uniformity of the LED surfaces are clearly displayed using color bars. The light intensity distribution of Ref-LED was considerably lower than those of the other LEDs. This is attributed to the poor current spreading of Ref-LED, in which most injected current was confined near the *p*-contact pad. By contrast, the light output intensity of the LEDs was improved by using ITO and AZO thin films, and the light output intensities of ITO-LED and AZO-LED were higher than that of Ref-LED. Furthermore, the distribution of light intensity in AZO-LED was considerably more uniform in the whole chip because of the enhanced current spreading by the AZO thin film. Figure 8(c) indicates that the AZO thin film was superior to the AuBe/Au electrode and ITO thin film regarding the current spreading ability.

The enhancement in light output intensity can be explained clearly by improved current spreading. Theoretically [14], the current spreading length (L_s) can be calculated using the following equation,

$$L_s = \sqrt{\frac{tn_{\text{ideal}}kT}{\rho J_0 q}} \quad (1)$$

where ρ and t are the resistivity and thickness of the current spreading layer, respectively. The k is the Boltzmann constant (1.38×10^{-23} J/K), and T is the absolute temperature, n_{ideal} is the diode ideality factor. The n_{ideal} of ITO-LED and AZO-LED are 1.68 and 1.37 in this study, respectively. The e is elementary charge and J_0 is the current density under metal. According Eq. (1), the current spreading ability can be enhanced by increased current spreading lengths, which were 72 μm and 180 μm for ITO- and AZO-LED. The large current spreading length of AZO-LED means the injection current will considerably more uniform to spread injection to whole chip. Then much more light can be extracted from the LED surface and there will be a reduction of re-absorbed light in the active layer of LED structure.

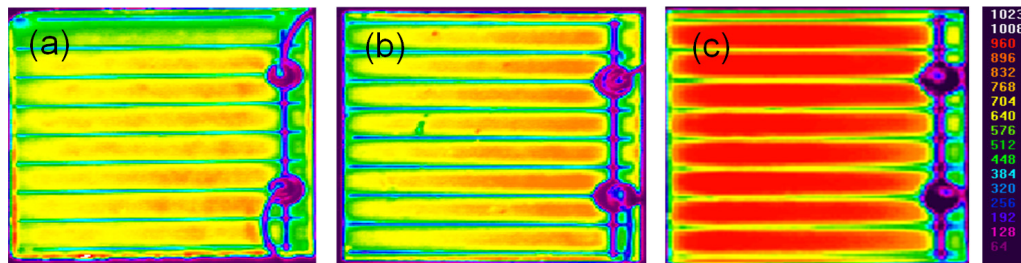


Fig. 8. Near-field optical images measured from (a) Ref- (b) ITO- and (c) AZO-LEDs.

Because driving electrical power into an LED can be transferred to optical output power and heat, the other performance evaluation of LED is the junction temperature. The junction temperature and output power of the Ref-, TCL-LEDs with different ambient temperature were measured and shown in Fig. 9. From Fig. 9(a), the junction temperature of the Ref-, ITO- and AZO-LEDs are 53.9°C, 35.8°C and 31.7°C at an ambient temperature of 25°C. Moreover, the junction temperatures of LEDs have significantly been improved by introducing the ITO and AZO thin films due to reduction of thermal accumulation. It means that the LEDs with TCL layer may be suitable for higher temperature operation. Figure 9(b) shows the results in the output power variation as a function of the ambient temperature. Obviously, the output powers of LEDs with ITO and AZO as a function of ambient temperature present much higher stability than that of Ref-LED. It is worth mentioning that the output power of AZO-LED was not only higher than those of Ref- and ITO-LEDs, but also exhibits better thermal stability than those of Ref- and ITO-LEDs.

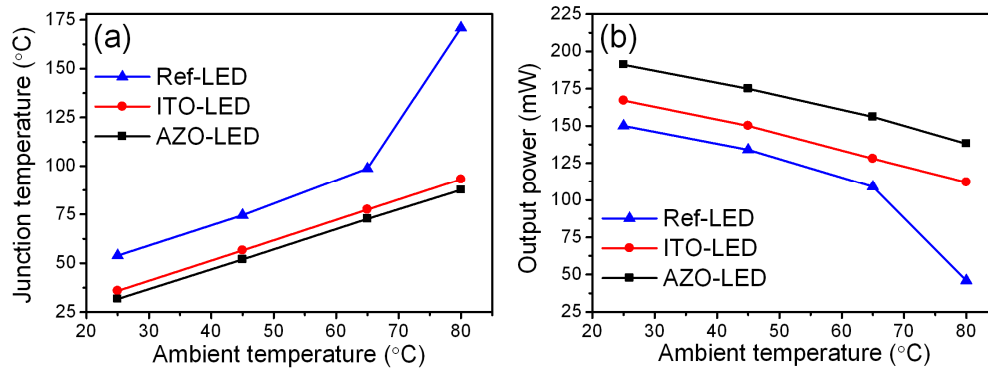


Fig. 9. (a) Junction temperature and (b) output power of the Ref-, ITO- and AZO-LEDs as function of ambient temperature under injection current of 350 mA.

4. Conclusion

This article reports on the performance of *p*-side-up thin-film AlGaInP LEDs containing thin carbon-doped GaP cap layers with ITO and AZO thin films. Compared with Ref-LED, ITO- and AZO-LEDs not only improved the light extraction efficiency, but also reduced the turn-on voltage of the LEDs. Due to refractive index of AZO being closer to the ideal refractive index between the GaP and epoxy layers than that of ITO, AZO extracted more light into the epoxy from the GaP layer than ITO did. Moreover, current spreading of AZO thin film in LED was better than that of the ITO thin film in LED. Therefore, AZO thin films prepared using ALD are potentially useful in AlGaInP LED applications and can reduce their manufacturing cost.

Acknowledgments

This study was financially supported by the Ministry of Science and Technology under contract numbers MOST 102-2221-E-005-071-MY3 and 104-2221-E-005-031-MY3, and Hsinchu Science Park and Southern Taiwan Science Park under contract numbers 101A08 and 102CE06, respectively.